Thermochromism of Metal Ion Complexes of Semiquinone Radical Anions. Control of Equilibria between Diamagnetic and Paramagnetic Species by Lewis Acids

Junpei Yuasa, Tomoyoshi Suenobu, and Shunichi Fukuzumi*

Department of Material and Life Science, Division of Advanced Science and Biotechnology, Graduate School of Engineering, Osaka University, SORST, Japan Science and Technology Agency (JST), Suita, Osaka 565-0871, Japan

Received: July 1, 2005; In Final Form: August 20, 2005

Metal ion complexes of semiquinone radical anions exhibit different types of thermochromism depending on metal ions and quinones. Metal ion complexes of 1,10-phenanthroline-5,6-dione radical anion ($PTQ^{\bullet-}$) produced by the electron-transfer reduction of PTQ by 1,1′-dimethylferrocene (Me_2Fc) in the presence of metal ions (Mg^{2+} and Sc^{3+}) exhibit the color change depending on temperature, accompanied by the concomitant change in the ESR signal intensity. In the case of Mg^{2+}, electron transfer from Me_2Fc to PTQ is in equilibrium, when the concentration of the $PTQ^{\bullet-}-Mg^{2+}$ complex ($\lambda_{max} = 486$ nm) increases with increasing temperature because of the positive enthalpy for the electron-transfer equilibrium. In contrast to the case of Mg^{2+}, electron transfer from Me_2Fc to PTQ is complete in the presence of Sc^{3+}, which is a much stronger Lewis acid than Mg^{2+}, to produce the $PTQ^{\bullet-}-Sc^{3+}$ complex ($\lambda_{max} = 631$ nm). This complex is in disproportionation equilibrium and the concentration of the $PTQ^{\bullet-}-Sc^{3+}$ complex increases with decreasing temperature because of the negative enthalpy for the proportionation direction, resulting in the remarkable color change in the visible region. On the other hand, the *p*-benzosemiquinone radical anion ($Q^{\bullet-}$) forms a 2:2 π-dimer radical anion complex $[Q^{\bullet-}-(Sc^{3+})_2-Q]$ with Q and Sc^{3+} ions at 298 K (yellow color), which is converted to a 2:3 π-dimer radical anion complex $[Q^{\bullet-}-(Sc^{3+})_3-Q]$ with a strong absorption band at $\lambda_{max} = 604$ nm (blue color) when the temperature is lowered to 203 K. The change in the number of binding Sc^{3+} ions depending on temperature also results in the remarkable color change, associated with the change in the ESR spectra.

Introduction

Thermochromic systems involving the change between paramagnetic and diamagnetic species have recently attracted considerable attention in relation to their potential applications in molecular devices.[1] Such paramagnetic compounds reported so far contain a redox active metal center and ligands.[2−11] A judicious choice of metal and ligands makes it possible to obtain thermally accessible low-lying electronic states that have considerable charge-transfer character, when thermally driven intramolecular electron transfer between the redox active metal and ligands (valence tautomerism) causes the reversible color change, associated with the change between the paramagnetic and diamagnetic states. A search for new valence tautomeric systems becomes an objective of current interest, because classic valence tautomeric complexes have been limited to transition metal complexes with redox active ligands.[2−11] In this context, an electroactive ferrocene derivative covalently linked to substituted triphenylmethyl radical has recently been reported to exhibit valence tautomerism, which is caused by thermally induced electron transfer from the electron donor moiety (the ferrocene unit) to the electron acceptor moiety (the organic radical unit).[12] Construction of such an electron donor−acceptor dyad exhibiting valence tautomerism has been extremely difficult, because fine-tuning of the redox potentials is required to attain the electron-transfer equilibrium.[12−15]

Organic radical anions are usually in equilibrium between the paramagnetic and diamagnetic species, e.g., an electron-transfer equilibrium between an electron donor (D) and an acceptor (A) in eq 1,[12−15] a disproportionation equilibrium of

$$D + A \rightleftarrows D^{\bullet+} + A^{\bullet-} \quad (1)$$

$$A^{\bullet-} + A^{\bullet-} \rightleftarrows A + A^{2-} \quad (2)$$

$$A^{\bullet-} + A \rightleftarrows (A)_2^{\bullet-} \quad (3)$$

$A^{\bullet-}$ in eq 2,[16] and an equilibrium between a paramagnetic monomer radical anion ($A^{\bullet-}$) and the dimer radical anion $(A)_2^{\bullet-}$ in eq 3.[17−19] Metal ions (M^{n+}) acting as Lewis acids accelerate electron-transfer reactions, when metal ions bind with the product radical anions.[20−26] The Lewis acidity of metal ions is directly correlated with the free energy change of electron-transfer reactions.[20−26] In such a case, appropriate choice of the metal ion would make it possible to regulate the equilibria between the paramagnetic and diamagnetic species (eqs 4−6).[20−26]

$$D + A \overset{M^{n+}}{\rightleftarrows} D^{\bullet+} + A^{\bullet-}-M^{n+} \quad (4)$$

$$A^{\bullet-}-M^{n+} + A^{\bullet-}-M^{n+} \underset{+M^{n+}}{\overset{-M^{n+}}{\rightleftarrows}} A + A^{2-}-M^{n+} \quad (5)$$

$$A^{\bullet-}-M^{n+} + A \rightleftarrows (A)_2^{\bullet-}-M^{n+} \quad (6)$$

The change in the equilibria between the paramagnetic and diamagnetic species depending on temperature would result in thermochromism, because organic radical ions normally possess low-lying excited states that exhibit strong color. As a conse-

* To whom correspondence should be addressed. E-mail: fukuzumi@chem.eng.osaka-u.ac.jp.

10.1021/jp053616p CCC: $30.25
Published on Web 09/27/2005

quence, the redox control of an organic electron acceptor by metal ions on the diamagnetic and paramagnetic equilibrium would expand the scope of the paramagnetic thermochromic systems. Despite such effective roles of metal ions on electron-transfer equilibria, there has been no systematic study on the effects of metal ions on the paramagnetic thermochromic systems.

We report herein new types of thermochromic systems using metal ion complexes of semiquinone radical anion ($Q^{\bullet-}$) and radical anion of 1,10-phenanthroline-5,6-dione ($PTQ^{\bullet-}$),[27] associated with the change in the ESR spectra.[29] The temperature dependence of the color and the ESR spectra is different depending on metal ions and quinones. The ESR measurements of the metal ion complexes of semiquinone radical anions, combined with the temperature-dependent UV−vis changes provide valuable insight into different mechanisms of the thermochromism for metal ion complexes of semiquinone radical anions.

Experimental Section

Materials. 1,10-Phenanthroline-5,6-dione (PTQ), *p*-benzoquinone (Q), and hydroquinone (QH_2) were obtained commercially and purified by the standard methods.[30] 1,1′-Dimethylferrocene (Me_2Fc) was obtained from Aldrich. Scandium triflate [$Sc(OTf)_3$] (OTf = OSO_2CF_3) was purchased from Pacific Metals Co., Ltd. (Taiheiyo Kinzoku). Decamethylferrocene (Fc*) was obtained from Wako Pure Chemical Co., Ltd. Anhydrous magnesium perchlorate [$Mg(ClO_4)_2$] was obtained from Nacalai Tesque. 2,2′-Diphenyl-1-picrylhydrazyl (DPPH) was obtained from Tokyo Kasei Organic Chemicals. Acetonitrile (MeCN) and propionitrile (EtCN) used as solvents were purified and dried by the standard procedure.[30]

ESR Measurements. Metal ion complexes of $PTQ^{\bullet-}$ were produced by the electron-transfer reduction of PTQ by Me_2Fc in the presence of metal ions. Typically, PTQ was dissolved in EtCN (7.8×10^{-4} M in 1.0 mL) in the presence of $Sc(OTf)_3$ (3.4×10^{-2} M) and purged with argon for 10 min. The PTQ solution (200 μL) and Me_2Fc solution (7.2×10^{-4} M in 200 μL) were introduced into the ESR cell (1.8 mm i.d.) and bubbled with Ar gas through a syringe that has a long needle. The $Q^{\bullet-}$−$(Sc^{3+})_n$−Q complexes (n = 2, 3) were produced by the proportionation equilibrium between Q and QH_2 in the presence of a high concentration of $Sc(OTf)_3$. Typically, Q (3.6×10^{-2} M) and QH_2 (6.4×10^{-3} M) were dissolved in EtCN (10 mL) and purged with argon for 10 min. $Sc(OTf)_3$ (6.4×10^{-1} M in 1.0 mL) was dissolved in deaerated EtCN. The Q solution (200 μL) and $Sc(OTf)_3$ solution (200 μL) were introduced into the ESR cell (1.8 mm i.d.) and were mixed by bubbling with Ar gas through a syringe with a long needle. ESR spectra were recorded on a JEOL JES-RE1XE spectrometer at the sample cell in the ESR cavity at various temperatures. The magnitude of modulation was chosen to optimize the resolution and signal-to-noise (S/N) ratio of the observed spectra under nonsaturating microwave power conditions. The g values were calibrated using an Mn^{2+} marker. The concentrations of radical species were determined by double integration of the ESR signal in reference to that of a known amount of a stable radical, DPPH. Typically, double integration of the ESR signal of a deaerated EtCN solution of Me_2Fc (3.6×10^{-4} M) and PTQ (3.9×10^{-4} M) in the presence of $Sc(OTf)_3$ (1.7×10^{-2} M) were compared with that of DPPH (2.0×10^{-4} M). The sensitivity of the ESR signals was corrected by using an Mn^{2+} marker as a reference.

Spectral Measurements. The temperature dependence of the absorption spectra of metal ion (Mg^{2+} and Sc^{3+}) complexes of semiquinone radical anions ($Q^{\bullet-}$ and $PTQ^{\bullet-}$) were examined from the change in the UV−vis spectra of metal ion complexes of semiquinone radical anions using a Hewlett-Packard 8453 diode array spectrophotometer at various temperatures.

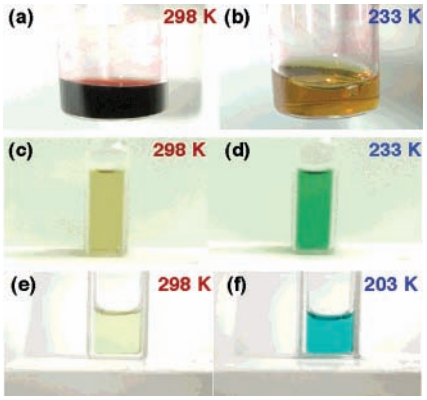

Figure 1. Photographs of a deaerated MeCN solution of Me_2Fc (2.0×10^{-2} M) and PTQ (2.0×10^{-2} M) in the presence of $Mg(ClO_4)_2$ (2.0×10^{-2} M) at (a) 298 K and (b) 233 K, photographs of a deaerated MeCN solution of Me_2Fc (2.4×10^{-4} M) and PTQ (2.5×10^{-3} M) in the presence of $Sc(OTf)_3$ (2.0×10^{-1} M) at (c) 298 K and (d) 233 K, and photographs of a deaerated EtCN solution of QH_2 (1.2×10^{-3} M) and Q (3.9×10^{-3} M) in the presence of $Sc(OTf)_3$ (5.4×10^{-1} M) at (e) 298 K and (f) 203 K.

Results and Discussion

Thermochromism of Metal Ion Complexes of Semiquinone Radical Anions. Metal ion (Mg^{2+} and Sc^{3+}) complexes of the 1,10-phenanthroline-5,6-dione radical anion ($PTQ^{\bullet-}$) were produced by the electron-transfer reduction of PTQ by 1,1′-dimethylferrocene (Me_2Fc) in the presence of metal ions (see the Experimental Section). The Sc^{3+} complex of the semiquinone radical anion ($Q^{\bullet-}$) is produced by the proportionation equilibrium between Q and hydroquinone (QH_2) in the presence of a high concentration of Sc^{3+} (see the Experimental Section).[29] The visible colors of the resulting solutions of the Mg^{2+} complex of $PTQ^{\bullet-}$, the Sc^{3+} complex of $PTQ^{\bullet-}$, and the Sc^{3+} complex of $Q^{\bullet-}$ at 298 K are shown in Figure 1a,c,e, respectively. Each color is changed when the temperature is lowered (Figure 1b,d,f). The color change can be repeated many times, being completely reversible.

The temperature-dependent reversible spectral changes were examined using propionitrile (EtCN) as a solvent that has a lower freezing point than acetonitrile (MeCN). The results are shown in Figure 2. The absorption band at λ_{max} = 486 nm due to the Mg^{2+} complex of $PTQ^{\bullet-}$ decreases with decreasing temperature (Figure 2a), whereas the absorption band at λ_{max} = 631 nm due to the Sc^{3+} complex of $PTQ^{\bullet-}$ increases when the temperature is lowered (Figure 2b). The temperature-dependent spectral change of the Sc^{3+} complex of $Q^{\bullet-}$ is shown in Figure 2c, where new absorption bands (λ_{max} = 374 and 604 nm) appear and the absorbance increases with decreasing temperature.

ESR Spectra of Metal Ion Complexes of Radical Anion. The ESR spectra of metal ion complexes of radical anions are measured at high and low temperatures, as shown in Figure 3 (red solid line and blue solid line, respectively). The ESR spectra of the Mg^{2+} complex of $PTQ^{\bullet-}$ measured in EtCN at 253 K (red solid line) and 203 K (blue solid line) are shown in Figure 3a, together with the computer simulation spectra (red broken lines) and the fitted values of the hyperfine splitting (hfs) constants and the maximum slope line width (ΔH_{msl}) for the

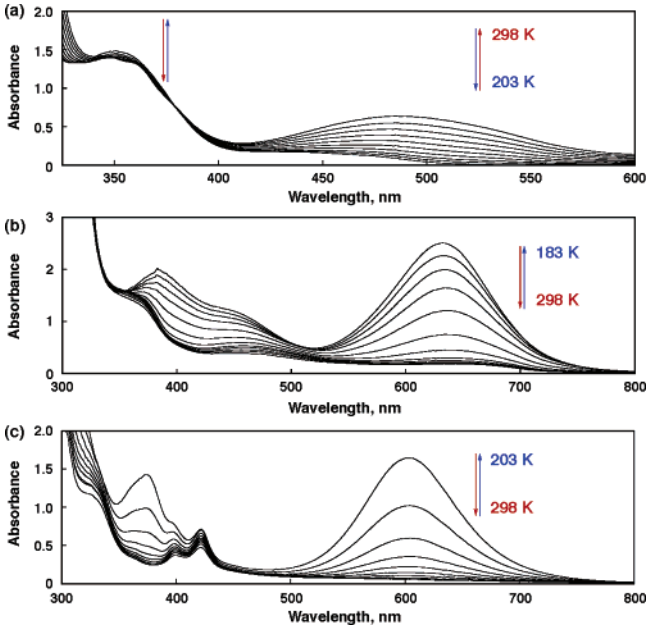

Figure 2. Absorption spectral changes of a deaerated EtCN solution of (a) Me_2Fc (1.7×10^{-3} M) and PTQ (1.7×10^{-3} M) in the presence of $Mg(ClO_4)_2$ (3.3×10^{-3} M) at various temperatures, those of (b) Me_2Fc (3.6×10^{-4} M) and PTQ (3.9×10^{-4} M) in the presence of $Sc(OTf)_3$ (1.7×10^{-2} M) at various temperatures, and those of (c) QH_2 (3.2×10^{-3} M) and Q (1.8×10^{-2} M) in the presence of $Sc(OTf)_3$ (3.2×10^{-1} M) at various temperatures (1 mm path length).

1:1 complex of Mg^{2+} with $PTQ^{\bullet-}$ ($PTQ^{\bullet-}-Mg^{2+}$). Only the high field part of the ESR spectrum is shown in Figure 3b−d to emphasize the complete agreement between the observed and simulated spectra (for the whole spectra, see Supporting Information S1). The ESR signal intensity of the $PTQ^{\bullet-}-Mg^{2+}$ complex decreases significantly when the temperature is lowered to 203 K (blue solid lines in Figure 3a,b), in agreement with the temperature dependence of the absorption at 486 nm in Figure 2a. The hfs values of the $PTQ^{\bullet-}-Mg^{2+}$ complex are slightly changed from those of free $PTQ^{\bullet-}$,[31,32] remaining the same at the lower temperature.

ESR spectra of the Sc^{3+} complex of $PTQ^{\bullet-}$ were also measured at 298 and 183 K, as shown in Figure 3c (solid lines). In contrast to the case of the $PTQ^{\bullet-}-Mg^{2+}$ complex in Figure 3a,b, the ESR signal intensity of the $PTQ^{\bullet-}-Sc^{3+}$ complex increases significantly when the temperature is lowered from 298 K (red solid line) to 183 K (blue solid line). This is also consistent with the temperature dependence of the absorption at 631 nm in Figure 2b. The hyperfine splitting due to four protons [$a(4H) = 0.126$ mT] and superhyperfine splitting due to Sc^{3+} ions [$a(Sc^{3+}) = 0.254$ mT] at 298 K (red solid line in Figure 3c) are slightly changed to the values of $a(4H) = 0.122$ mT and $a(Sc^{3+}) = 0.270$ mT at 183 K (blue solid line in Figure 3c).

The ESR spectrum of the Sc^{3+} complex of $Q^{\bullet-}$ at 298 K (red solid line in Figure 3d) is changed drastically together with an increase in the signal intensity when the temperature is lowered to 203 K (blue solid line in Figure 3d). This shows a sharp contrast to the case of ESR spectra of metal ion complexes of $PTQ^{\bullet-}$ where the hyperfine patterns remain virtually the same at different temperatures. The ESR spectrum observed at 298 K (red solid line in Figure 3d) with the hyperfine splitting due to eight equivalent protons [$a(8H) = 0.112$ mT] and superhyperfine splitting due to two equivalent Sc^{3+} ions [$a(2Sc^{3+}) = 0.112$ mT] agrees with that of the π-dimer formed between $Q^{\bullet-}$ and Q, which is bridged by two equivalent Sc^{3+} ions [$Q^{\bullet-}-(Sc^{3+})_2-Q$].[26,29] When the temperature is lowered to 203 K, the ESR spectrum is changed to exhibit further superhyperfine splitting due to an additional Sc^{3+} ion [$a(Sc^{3+}) = 0.075$ mT] (blue sold line in Figure 3d). The ESR spectrum agrees with that of $Q^{\bullet-}-(Sc^{3+})_3-Q$ in which additional Sc^{3+} is placed between the π-planes of $Q_2^{\bullet-}$ to produce $Q^{\bullet-}-(Sc^{3+})_3-Q$.[26,29] The change in the ESR spectrum between $Q^{\bullet-}-(Sc^{3+})_2-Q$ and $Q^{\bullet-}-(Sc^{3+})_3-Q$ was reversible, as observed in the color change in Figure 2c. The decrease in the number of binding Sc^{3+} ions from 3 to 2 is clearly recognized as the disappearance of the ESR signal at the lowest or highest magnetic field region due to the loss of additional superhyperfine splitting due to one Sc^{3+} ion with increasing temperature (Figure 3d).

To confirm the assignment of the absorption bands due to metal ion complexes of radical anions, the concentrations of metal ion complexes of radical anions were determined by double integration of the ESR signal in reference to that of a known amount of a stable radical, 2,2′-diphenyl-1-picrylhydrazyl (DPPH), under the same experimental conditions as employed for the color change in Figure 2 at various temperatures. The concentration of the Mg^{2+} complex of $PTQ^{\bullet-}$ determined by ESR increases with increasing temperature (open circles in Figure 4a) and this agrees with an increase in absorbance at 486 nm (closed circles in Figure 4a) using the molecular absorption coefficient (ϵ) value of $PTQ^{\bullet-}-Mg^{2+}$ at 486 nm (4.5×10^3 M^{-1} cm^{-1}). In the case of the Sc^{3+} complex of $PTQ^{\bullet-}$, the radical concentration decreases with increasing temperature (open circles in Figure 4b). This also agrees with a decrease in absorbance at 631 nm (closed circles in Figure 4b) using the ϵ value of $PTQ^{\bullet-}-Sc^{3+}$ at 631 nm (4.2×10^4 M^{-1} cm^{-1}). The agreement between the change in the radical concentration and the absorbance change in Figure 4a,b indicates that the temperature dependence of the absorption spectra in Figure 2a and Figure 2b results from the change in the concentrations of metal ion complexes of $PTQ^{\bullet-}$.[33]

The total concentrations of $Q^{\bullet-}-(Sc^{3+})_2-Q$ and $Q^{\bullet-}-(Sc^{3+})_3-Q$ also decrease with increasing temperature (open circles in Figure 4c). In this case, however, the radical concentration remains the same at high temperatures (open circles in Figure 4c), whereas the absorbance at 604 nm decreases to zero at high temperatures (closed circles in Figure 4c). The ϵ value of $Q^{\bullet-}-(Sc^{3+})_3-Q$ at 604 nm is determined as 3.3×10^4 M^{-1} cm^{-1} from the radical concentration and the absorbance at 604 nm at 203 K, because $Q^{\bullet-}-(Sc^{3+})_3-Q$ is the main radical species at 203 K, as indicated by the ESR spectrum of $Q^{\bullet-}-(Sc^{3+})_3-Q$ obtained at 203 K (Figure 3d). When the temperature dependence of the ESR signal intensity due to $Q^{\bullet-}-(Sc^{3+})_3-Q$ at 331.28 mT (open circles in Figure 5) agrees well with that of the absorbance at 604 nm (closed circles in Figure 5), this indicates that the temperature dependence of the absorption spectra in Figure 2c results from the change in the number of binding Sc^{3+} ions between 2 for [$Q^{\bullet-}-(Sc^{3+})_2-Q$] and 3 for [$Q^{\bullet-}-(Sc^{3+})_3-Q$] with temperature. Thus, there are two equilibria: one is between QH_2 and Q in the presence of a large concentration of Sc^{3+}, and the other is between $Q^{\bullet-}-(Sc^{3+})_2-Q$ and $Q^{\bullet-}-(Sc^{3+})_3-Q$ as shown in Scheme 1. The latter is responsible for the color change in Figures 1e and 1f.

The absorption band due to the dimer radical anion ($Q_2^{\bullet-}$) without Sc^{3+} appears at $\lambda_{max} = 1290$ nm in the NIR (near-infrared) region.[29,34] This is assigned to the transition from the π-bonding orbital of the π-dimer to the π^* orbital (see Supporting Information S2).[19,29] Thus, the λ_{max} value varies depending on the π-bonding strength. The binding of two Sc^{3+}

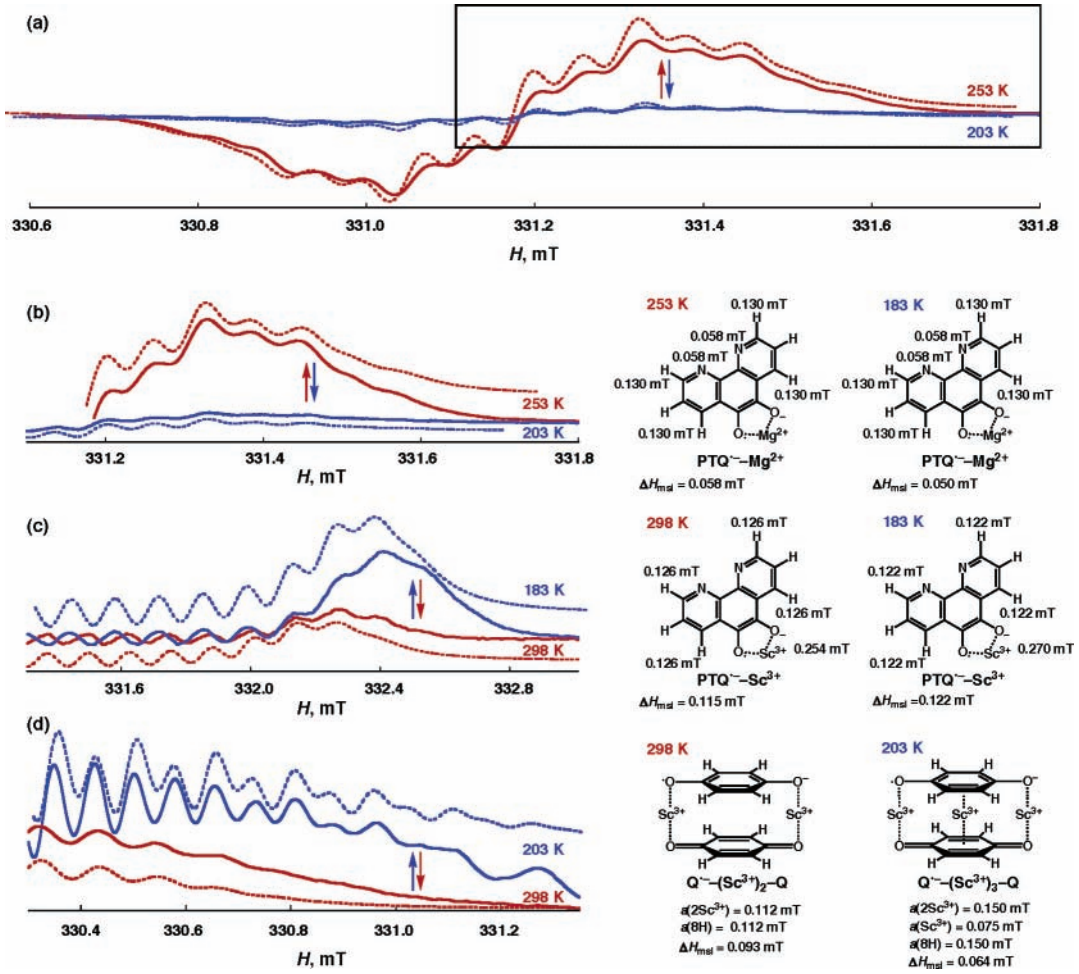

Figure 3. ESR spectra of a deaerated EtCN solution of (a) Me_2Fc (1.7×10^{-2} M) and PTQ (1.8×10^{-2} M) in the presence of $Mg(ClO_4)_2$ (5.1×10^{-2} M) in the magnetic range 330.60−331.80 mT at 253 K (red solid line) and 203 K (blue solid line) with the computer simulation spectra of $PTQ^{\bullet-}-Mg^{2+}$ at 253 K (red broken line) and 203 K (blue broken line) [the boxed area is magnified and shown in Figure 3b] and (b) those at the magnetic range 331.10−331.80 mT. (c) ESR spectra of a deaerated EtCN solution of Me_2Fc (3.6×10^{-4} M) and PTQ (3.9×10^{-4} M) in the presence of $Sc(OTf)_3$ (4.0×10^{-1} M) in the magnetic range 331.31−333.01 mT at 298 K (red solid line) and 183 K (blue solid line) with the computer simulation spectra of $PTQ^{\bullet-}-Sc^{3+}$ at 298 K (red broken line) and 183 K (blue broken line). (d) ESR spectra of a deaerated EtCN solution of QH_2 (3.2×10^{-3} M) and Q (1.8×10^{-2} M) in the presence of $Sc(OTf)_3$ (3.2×10^{-1} M) in the magnetic range 330.30−331.35 mT at 298 K (red solid line) and 203 K (blue solid line) with the computer simulation spectra of $Q^{\bullet-}-(Sc^{3+})_2-Q$ (red broken line) and $Q^{\bullet-}-(Sc^{3+})_3-Q$ (blue broken line). The hfs values are given at the right-hand side with the structures of the metal ion complexes of radical anions. Red and blue arrows denote an increase and decrease in temperature, respectively.

ions with $Q_2^{\bullet-}$ results in an increase in the π-bonding strength, leading to a significant blue shift of the absorption band of the π-complex. The additional binding of Sc^{3+} between the two π-planes of $Q_2^{\bullet-}$, which has Coulombic rather than covalent character, may decrease the π-bonding strength, resulting in the red-shift of the absorption band, as observed in Figure 2c.

Mechanism of Thermochromism of Metal Ion Complexes of $PTQ^{\bullet-}$. To clarify the difference in thermochromism between the Mg^{2+} and Sc^{3+} complexes of $PTQ^{\bullet-}$, spectral titration of PTQ by ferrocenes is examined. The absorption changes due to the complex formation of $PTQ^{\bullet-}$ with metal ions are shown in Figure 6. The change of absorbance at 631 nm due to the $PTQ^{\bullet-}-Sc^{3+}$ complex is observed upon addition of Me_2Fc (0−3.2×10^{-3} M) to a deaerated MeCN solution of PTQ (1.5×10^{-3} M) (closed circles in Figure 6a), and this agrees with the concentration of the $PTQ^{\bullet-}-Sc^{3+}$ complex determined by ESR (open circles in Figure 6a).[35] The concentration of the $PTQ^{\bullet-}-Sc^{3+}$ complex reaches a maximum (12%) after the 1:1 ratio of Me_2Fc to PTQ and then decreases with increasing concentration of Me_2Fc (open circles in Figure 6a).[35] This indicates that the $PTQ^{\bullet-}-Sc^{3+}$ complex formed in electron transfer from Me_2Fc to PTQ in the presence of Sc^{3+} (eq 7) is further reduced by

$$Me_2Fc + PTQ \underset{-Sc^{3+}}{\overset{+Sc^{3+}}{\rightleftarrows}} Me_2Fc^+ + PTQ^{\bullet-}-Sc^{3+} \quad (7)$$

$$Me_2Fc + PTQ^{\bullet-}-Sc^{3+} \rightleftarrows Me_2Fc^+ + PTQ^{2-}-Sc^{3+} \quad (8)$$

$$PTQ^{2-}-Sc^{3+} + PTQ \underset{-Sc^{3+}}{\overset{+Sc^{3+}}{\rightleftarrows}} 2PTQ^{\bullet-}-Sc^{3+} \quad (9)$$

excess Me_2Fc to produce $PTQ^{2-}-Sc^{3+}$ (eq 8) and that the $PTQ^{\bullet-}-Sc^{3+}$ complex is in disproportionation equilibrium with the $PTQ^{2-}-Sc^{3+}$ complex and PTQ (eq 9). It should be noted that the electron-transfer equilibrium (eq 7) largely lies on the side of the Me_2Fc^+ and $PTQ^{\bullet-}-Sc^{3+}$ under the present experimental conditions, because the free energy change of electron transfer from Me_2Fc ($E^0_{ox} = 0.26$ V vs SCE)[36] to PTQ ($E_{red} = 0.31$ V vs SCE in the presence of 2.0×10^{-2} M Sc^{3+})[37] is negative ($\Delta G_{et} = -0.05$ eV).[38]

In the case of Mg^{2+}, which is a much weaker Lewis acid than Sc^{3+}, the absorbance at 486 nm (closed triangles in Figure

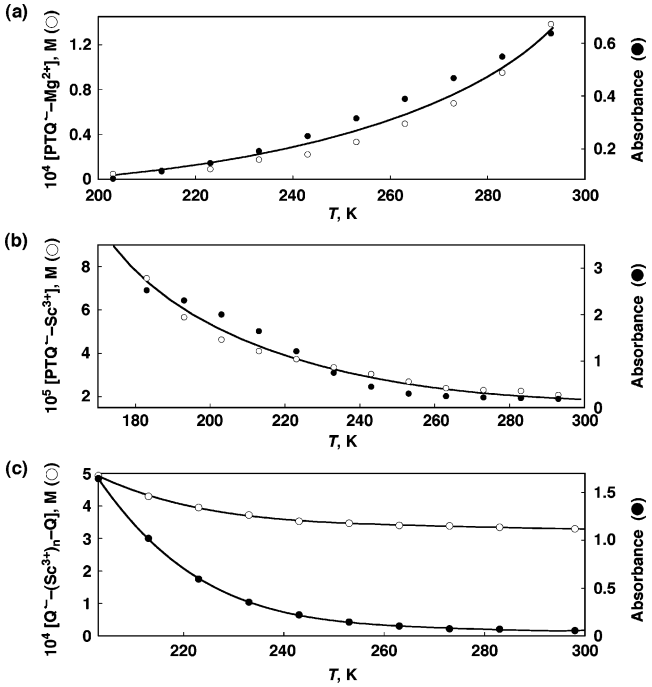

Figure 4. Plots of (a) concentration of $PTQ^{\bullet-}-Mg^{2+}$ (○) and absorbance at 486 nm (●) vs T in the deaerated EtCN solution of Me_2Fc (1.7×10^{-3} M) and PTQ (1.7×10^{-3} M) in the presence of $Mg(ClO_4)_2$ (3.3×10^{-3} M) at 203−298 K. (b) Plots of the concentration of $PTQ^{\bullet-}-Sc^{3+}$ (○) and absorbance at 631 nm (●) vs T in the deaerated EtCN solution of Me_2Fc (3.6×10^{-4} M) and PTQ (3.9×10^{-4} M) in the presence of $Sc(OTf)_3$ (1.7×10^{-2} M) at 183−298 K. (c) Plots of total concentrations of $Q^{\bullet-}-(Sc^{3+})_n-Q$ ($n = 2$, 3) (○) and absorbance at 604 nm (●) (1 mm path length) vs T in the deaerated EtCN solution of QH_2 (3.2×10^{-3} M) and Q (1.8×10^{-2} M) in the presence of $Sc(OTf)_3$ (3.2×10^{-1} M) at 203−298 K.

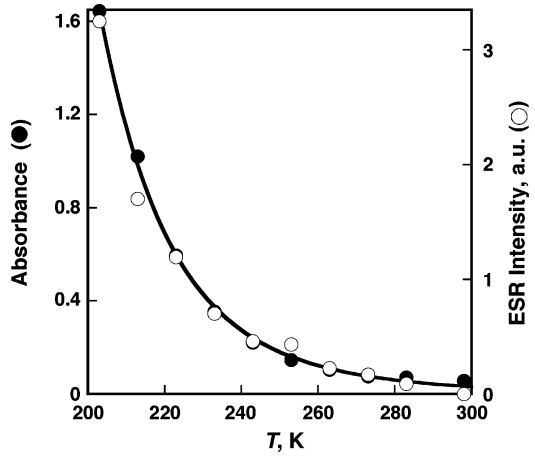

Figure 5. Temperature dependence of the ESR intensity at 331.28 mT (○) and the absorbance at 604 nm (●) (1 mm path length) of an EtCN solution of QH_2 (3.2×10^{-3} M) and Q (1.8×10^{-2} M) in the presence of $Sc(OTf)_3$ (3.2×10^{-1} M) at 298−203 K.

SCHEME 1

$$QH_2 + Q \underset{2Q,\ 4Sc^{3+}\ 2H^+}{\overset{2Q,\ 4Sc^{3+}\ 2H^+}{\rightleftharpoons}} 2[Q^{\bullet-}-(Sc^{3+})_2-Q] \underset{-2Sc^{3+}}{\overset{+2Sc^{3+}}{\rightleftharpoons}} 2[Q^{\bullet-}-(Sc^{3+})_3-Q]$$

6b) and the concentration of the $PTQ^{\bullet-}-Mg^{2+}$ complex determined by ESR (open triangles in Figure 6b) continue to increase with increasing concentration of Me_2Fc even after the 1:1 ratio of Me_2Fc to PTQ is reached. This indicates that electron

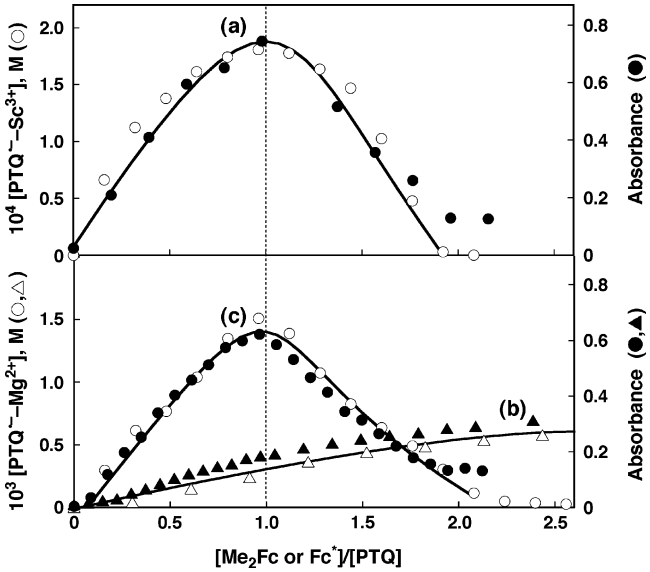

Figure 6. Plots of (a) concentration of $PTQ^{\bullet-}-Sc^{3+}$ (○) and absorbance at 631 nm (●) (1 mm path length) vs [Me_2Fc]/[PTQ] for the titration of PTQ (1.5×10^{-3} M) by Me_2Fc (0−3.2×10^{-3} M) in the presence of $Sc(OTf)_3$ (2.0×10^{-1} M) in deaerated MeCN at 243 K, (b) concentration of $PTQ^{\bullet-}-Mg^{2+}$ (△) and absorbance at 486 nm (▲) (1 mm path length) vs [Me_2Fc]/[PTQ] for the titration of PTQ (1.6×10^{-3} M) by Me_2Fc (0−3.8×10^{-3} M) in the presence of $Mg(ClO_4)_2$ (1.9×10^{-2} M) in deaerated MeCN at 298 K, and (c) concentration of $PTQ^{\bullet-}-Mg^{2+}$ (○) and absorbance at 486 nm (●) (1 mm path length) vs [Fc*]/[PTQ] for the titration of PTQ (1.6×10^{-3} M) by Fc* (0−4.2×10^{-3} M) in the presence of $Mg(ClO_4)_2$ (1.9×10^{-2} M) in deaerated MeCN at 298 K.

transfer between Me_2Fc and PTQ is in equilibrium in the presence of Mg^{2+} at 298 K, as shown in eq 10.

$$Me_2Fc + PTQ \underset{-Mg^{2+}}{\overset{+Mg^{2+}}{\rightleftharpoons}} Me_2Fc^+ + PTQ^{\bullet-}-Mg^{2+} \quad (10)$$

When decamethylferrocene (Fc*: $E^0_{ox} = -0.08$ V vs SCE),[36] which is a much stronger electron donor than Me_2Fc ($E^0_{ox} = 0.26$ V vs SCE),[36] was used as an electron donor, the electron-transfer equilibrium is completely shifted to the product side to afford 98% yield of the $PTQ^{\bullet-}-Mg^{2+}$ complex at a 1:1 ratio of Fc* to PTQ (open circles in Figure 6c) and then decreases with increasing concentration of Fc*. This indicates that the disproportionation equilibrium of the $PTQ^{\bullet-}-Mg^{2+}$ complex largely lies on the side of the $PTQ^{\bullet-}-Mg^{2+}$ complex (the direction toward the proportionation), as shown in eq 11.

$$PTQ^{2-}-Mg^{2+} + PTQ \underset{-Mg^{2+}}{\overset{+Mg^{2+}}{\rightleftharpoons}} 2PTQ^{\bullet-}-Mg^{2+} \quad (11)$$

The opposite temperature dependence between the $PTQ^{\bullet-}-Sc^{3+}$ complex and the $PTQ^{\bullet-}-Mg^{2+}$ complex in Figure 4 results from the difference in the sign of enthalpy (ΔH) between the proportionation equilibrium (eq 9) with $\Delta H = -3.0$ kcal mol^{-1} and the electron-transfer equilibrium (eq 10) with $\Delta H = 9.0$ kcal mol^{-1} (see Supporting Information S3 for plots of logarithm of the equilibrium constants vs T^{-1}). The decrease in absorbance at 604 nm and the ESR signal intensity due to $Q^{\bullet-}-(Sc^{3+})_3-Q$ at 331.28 mT with increasing temperature in Figure 5 is also ascribed to the negative enthalpy for formation of $Q^{\bullet-}-(Sc^{3+})_3-Q$ because of the additional binding of Sc^{3+}.

Summary and Conclusions

Three different types of thermochromism have been shown in paramagnetic systems involving metal ion complexes of

semiquinone radical anions. The *p*-benzosemiquinone radical anion ($Q^{\bullet-}$) forms 2:2 π-dimer radical anion complex [$Q^{\bullet-}-(Sc^{3+})_2-Q$] with Q and Sc^{3+} ion at 298 K (yellow color), which changes to a 2:3 π-dimer radical anion complex [$Q^{\bullet-}-(Sc^{3+})_3-Q$] when the temperature is lowered to 203 K, which has a strong absorption band at 604 nm (blue color). Metal ion complexes of 1,10-phenanthroline-5,6-dione radical anion ($PTQ^{\bullet-}$) were produced by the electron-transfer reduction of PTQ by 1,1′-dimethylferrocene (Me_2Fc) in the presence of metal ions (Mg^{2+} and Sc^{3+}). In the case of Mg^{2+}, electron transfer from Me_2Fc to PTQ is in equilibrium, when the concentration of the $PTQ^{\bullet-}-Mg^{2+}$ complex increases with increasing temperature, leading to an increase in the absorption band ($\lambda_{max} = 486$ nm). On the other hand, electron transfer from Me_2Fc to PTQ is complete in the presence of Sc^{3+}, which is a much stronger Lewis acid than Mg^{2+}. The $PTQ^{\bullet-}-Sc^{3+}$ complex thus produced is in disproportionation equilibrium and the concentration of the $PTQ^{\bullet-}-Sc^{3+}$ complex increases with decreasing temperature because of the negative enthalpy for the proportionation. This causes the remarkable color change in the visible region ($\lambda_{max} = 631$ nm).

Acknowledgment. This work was partially supported by Grants-in-Aid (Nos. 16205020 and 17550058) from the Ministry of Education, Culture, Sports, Science and Technology, Japan.

Supporting Information Available: ESR spectra of [$Q^{\bullet-}-(Sc^{3+})_n-Q$] ($n = 2$, 3) and $PTQ^{\bullet-}-Sc^{3+}$ at high and low temperature (S1), NIR spectra of $Q_2^{\bullet-}$ and determination of the formation constant of $Q_2^{\bullet-}$ (S2), and plots of logarithm of the equilibrium constants vs T^{-1} (S3). This material is available free of charge via the Internet at http://pubs.acs.org.

References and Notes

(1) (a) Crano, J. C.; Guglielmetti, R. *Organic Photochromic and Thermochromic Compounds*; Plenum Press: New York, 1999. (b) *Molecular Switches*; Ferringa, B. L., Ed.; Wiley-VCH: Weinheim, 2001. (c) Kahn, O.; Jay, C. *Science* **1998**, *279*, 44.

(2) (a) Adams, D. M.; Dei, A.; Rheingold, A. L.; Hendrickson, D. N. *J. Am. Chem. Soc.* **1993**, *115*, 8221. (b) Adams D. M.; Hendrickson, D. N. *J. Am. Chem. Soc.* **1996**, *118*, 11515. (c) Adams, D. M.; Li, B. L.; Simon, J. D.; Hendrickson, D. N. *Angw. Chem., Int. Ed. Engl.* **1995**, *34*, 1481. (d) Ruiz, D.; Yoo, J.; Guzei, I.; Rheingold, A.; Hendrickson, D. N. *Chem. Commun.* **1998**, 2089.

(3) (a) Caneschi, A.; Cornia, A.; Dei, A. *Inorg. Chem.* **1998**, *37*, 3419. (b) Ruiz-Molina, D.; Veciana, J.; Wurst, K.; Hendrickson, D. N.; Rovira, C. *Inorg. Chem.* **2000**, *39*, 617. (c) Speier, G.; Tyeklar, Z.; Toth, P.; Speier, E.; Tisza, S.; Rockenbauer, A.; Whalen, A. M.; Alkire, N.; Pierpont, C. G. *Inorg. Chem.* **2001**, *40*, 5653.

(4) Bin-Salamon, S.; Brewer, S.; Franzen, S.; Feldheim, D. L.; Lappi, S.; Shultz, D. A. *J. Am. Chem. Soc.* **2005**, *127*, 5328.

(5) (a) Pierpont, C. G. *Coord. Chem. Rev.* **2001**, *219*−*221*, 415. (b) Pierpont, C. G.; Lange, C. W. *Prog. Coord. Chem.* **1993**, *41*, 381. (c) Shultz, D. A. In *Magnetoscience-From Molecules to Materials*; Miller, J. S., Drillon, M., Eds.; Wiley-VCH: New York, 2000.

(6) (a) Attia, A. S.; Pierpont, C. G. *Inorg. Chem.* **1995**, *34*, 1172. (b) Attia, A. S.; Pierpont, C. G. *Inorg. Chem.* **1998**, *37*, 3051. (c) Attia, A. S.; Pierpont, C. G. *Inorg. Chem.* **1997**, *36*, 6184.

(7) Shaikh, N.; Goswami, S.; Panja, A.; Wang, X.-Y.; Gao, S.; Butcher, R. J.; Banerjee, P. *Inorg. Chem.* **2004**, *43*, 5908.

(8) (a) Shimazaki, Y.; Tani, F.; Fukui, K.; Naruta, Y.; Yamauchi, O. *J. Am. Chem. Soc.* **2003**, *125*, 10512. (b) Shimazaki, Y.; Huth, S.; Karasawa, S.; Hirota, S.; Naruta, Y.; Yamauchi, O. *Inorg. Chem.* **2004**, *43*, 7816. (c) Seth, J.; Palaniappan, V.; Bocian, D. F. *Inorg. Chem.* **1995**, *34*, 2201.

(9) Helton, M. E.; Gebhart, N. L.; Davies, E. S.; McMaster, J.; Garner, C. D.; Kirk, M. L. *J. Am. Chem.* Soc. **2001**, *123*, 10389.

(10) (a) Rall, J.; Wanner, M.; Albrecht, M.; Hornung, F. M.; Kaim, W. *Chem.-Eur. J.* **1999**, *5*, 2802. (b) Speier, G.; Tyeklar, Z.; Toth, P.; Speier, E.; Tisza, S.; Rockenbauer, A.; Whalen, A. M.; Alkire, N.; Pierpont, C. G. *Inorg. Chem.* **2001**, *40*, 5653.

(11) Ghumaan, S.; Sarkar, B.; Patra, S.; van Slageren, J.; Fiedler, J.; Kaim, W.; Lahiri, G. K. *Inorg. Chem.* **2005**, *44*, 3210.

(12) Ratera, I.; Ruiz-Molina, D.; Renz, F.; Ensling, J.; Wurst, K.; Rovira, C.; Gütlich, P.; Veciana, J. *J. Am. Chem. Soc.* **2003**, *125*, 1462.

(13) (a) Perepichka, D. F.; Bryce, M. R.; Pearson, C.; Petty, M. C.; McInnes, E. J. L.; Zhao, J. P. *Angew. Chem., Int. Ed.* **2003**, *42*, 4636. (b) Perepichka, D. F.; Bryce, M. R.; Batsanov, A., S.; McInnes, E. J. L.; Zhao, J. P.; Farley, R. D. *Chem.-Eur. J.* **2002**, *8*, 4656. (c) Perepichka, D. F.; Bryce, M. R.; Perepichka, I. F.; Lyubchik, S. B.; Christensen, C. A.; Godbert, N.; Batsanov, A. S.; Levillain, E.; McInnes, E. J. L.; Zhao, J. P. *J. Am. Chem. Soc.* **2002**, *124*, 14227.

(14) (a) Mizuno, K.; Kurihara, M.; Takagi, S.; Nishihara, H. *Chem. Lett.* **2003**, 788. (b) Murata, M.; Yamada, M.; Fujita, T.; Kojima, K.; Kurihara, M.; Kubo, K.; Kobayashi, Y.; Nishihara, H. *J. Am. Chem. Soc.* **2001**, *123*, 12903.

(15) Lopez, J. L.; Tárraga, A.; Espinosa, A.; Velasco, M. D.; Molina, P.; Lloveras, V.; Vidal-Gancedo, J.; Rovira, C.; Veciana, J.; Evans, D. J.; Wurst, K. *Chem.-Eur. J.* **2004**, *10*, 1815.

(16) Itoh, S.; Kawakami, H.; Fukuzumi, S. *J. Am. Chem. Soc.* **1998**, *120*, 7271.

(17) Tolbert, L. M.; Solntsev, K. M. *Acc. Chem. Res.* **2002**, *35*, 19.

(18) (a) Lü, J.-M.; Rosokha, S. V.; Kochi, J. K. *J. Am. Chem. Soc.* **2003**, *125*, 12161. (b) Small, D.; Zaitsev, V.; Jung, Y.; Rosokha, S. V.; Head-Gordon, M.; Kochi, J. K. *J. Am. Chem. Soc.* **2004**, *126*, 13850. (c) Kochi, J. K.; Rathore, R.; Magueres, P. L. *J. Org. Chem.* **2000**, *65*, 6826. (d) Lü, J.-M.; Rosokha, S. V.; Lindeman, S. V.; Neretin, I. S.; Kochi, J. K. *J. Am. Chem. Soc.* **2005**, *127*, 1797. (e) Davlieva, M. G.; Lü, J.-M.; Lindeman, S. V.; Kochi, J. K. *J. Am. Chem. Soc.* **2004**, *126*, 4557.

(19) Paramagnetic radical anions are also in equilibrium with diamagnetic dimer dianion; see: Del Sesto, R. E.; Miller, J. S.; Lafuente, P.; Novoa, J. J. *Chem.-Eur. J.* **2002**, *8*, 4894.

(20) (a) Fukuzumi, S. In *Electron Transfer in Chemistry*; Balzani, V., Ed.; Wiley-VCH: Weinheim, 2001; Vol. 4, pp 3−67. (b) Fukuzumi, S. *Org. Biomol. Chem.* **2003**, *1*, 609. (c) Fukuzumi, S. *Bull. Chem. Soc. Jpn.* **1997**, *70*, 1.

(21) (a) Fukuzumi, S.; Ohkubo, K. *Chem.-Eur. J.* **2000**, *6*, 4532. (b) Ohkubo, K.; Menon, S. C.; Orita, A.; Otera, J.; Fukuzumi, S. *J. Org. Chem.* **2003**, *68*, 4720.

(22) (a) Ohkubo, K.; Suenobu, T.; Imahori, H.; Orita, A.; Otera, J.; Fukuzumi, S. *Chem. Lett.* **2001**, 978. (b) Ohtsu, H.; Fukuzumi, S. *Chem.-Eur. J.* **2001**, *7*, 4947. (c) Fukuzumi, S.; Ohkubo, K. *J. Am. Chem. Soc.* **2002**, *124*, 10270.

(23) (a) Fukuzumi, S.; Ohkubo, K.; Okamoto, T.; *J. Am. Chem. Soc.* **2002**, *124*, 14147. (b) Fukuzumi, S.; Fujii, Y.; Suenobu, T. *J. Am. Chem. Soc.* **2001**, *123*, 10191. (c) Fukuzumi, S.; Yuasa, J.; Suenobu, T. *J. Am. Chem. Soc.* **2002**, *124*, 12566.

(24) (a) Fukuzumi, S.; Okamoto, K.; Imahori, H. *Angew. Chem., Int. Ed.* **2002**, *41*, 620. (b) Fukuzumi, S.; Yoshida, Y.; Okamoto, K.; Imahori, H.; Araki, Y.; Ito, O. *J. Am. Chem. Soc.* **2002**, *124*, 6794. (c) Fukuzumi, S.; Okamoto, K.; Yoshida, Y.; Imahori, H.; Araki, Y.; Ito, O. *J. Am. Chem. Soc.* **2003**, *125*, 1007.

(25) Itoh, S.; Taniguchi, M.; Takada, N.; Nagatomo, S.; Kitagawa, T.; Fukuzumi, S. *J. Am. Chem. Soc.* **2000**, *122*, 12087.

(26) Yuasa, J.; Suenobu, T.; Fukuzumi, S. *J. Am. Chem. Soc.* **2003**, *125*, 12090.

(27) PTQ was chosen as a representative of *o*-quinones in this work, because the reduction potential of PTQ ($E^0_{red} = -0.48$ V vs SCE) is close to that of *p*-benzoquinone ($E^0_{red} = -0.51$ V vs SCE).[28]

(28) Fukuzumi, S.; Koumitsu, S.; Hironaka, K.; Tanaka, T. *J. Am. Chem. Soc.* **1987**, *109*, 305.

(29) A part of the present results has appeared as a preliminary communication; see: Yuasa, J.; Fukuzumi, S. *Org. Biomol. Chem.* **2004**, *2*, 642.

(30) Armarego, W. L. F.; Perrin, D. D. *Purification of Laboratory Chemicals*, 4th ed.; Butterworth-Heinemann: Boston, 1996.

(31) $PTQ^{\bullet-}$ was produced by photoinduced electron transfer from dimeric 1-benzyl-1,4-dihydronicotinamide [$(BNA)_2$][32] to PTQ. The hyperfine splittings due to six protons [a(4H) = 0.132 mT and a(2H) = 0.024 mT] and two equivalent nitrogens [a(2N) = 0.057 mT] of $PTQ^{\bullet-}$ are only slightly changed by the complex formation with Mg^{2+}.

(32) (a) Patz, M.; Kuwahara, Y.; Suenobu, T.; Fukuzumi, S. *Chem. Lett.* **1997**, 567. (b) Fukuzumi, S.; Suenobu, T.; Patz, M.; Hirasaka, T.; Itoh, S.; Fujitsuka, M.; Ito, O. *J. Am. Chem. Soc.* **1998**, *120*, 8060.

(33) The opposite temperature dependence of concentrations of the $PTQ^{\bullet-}-Mg^{2+}$ and $PTQ^{\bullet-}-Sc^{3+}$ complexes is also observed when the concentrations of Mg^{2+} (3.3×10^{-3} M) and Sc^{3+} (1.7×10^{-2} M) were increased to 3.3×10^{-2} M and 4.0×10^{-1} M, respectively. Thus, the opposite temperature dependence is not caused by the difference in the concentrations of metal ions.

(34) The formation constant of $Q_2^{\bullet-}$ is determined as 9.7 M^{-1} at 298 K (see Supporting Information S2). For NIR bands due to other dimer radical anions, see: Ganesan, V.; Rosokha, S. V.; Kochi, J. K. *J. Am. Chem. Soc.* **2003**, *125*, 2559. Diamagnetic dimers of metal ion complexes of 9,10-phenanthrenequinone radical anion were reported previously; see: Staples, T. L.; Szwarc, M. *J. Am. Chem. Soc.* **1970**, *92*, 5022.

(35) The absorbance at 631 nm plotted in Figure 6a does not reach zero at 2:1 ratio of Me_2Fc to PTQ, because ferricenium cation (Me_2Fc^+) formed in the electron transfer has small absorption at 631 nm.

(36) Fukuzumi, S.; Mochizuki, S.; Tanaka, T. *Inorg. Chem.* **1989**, *28*, 2459.

(37) The E_{red} value of PTQ in the absence of metal ion (−0.48 V vs SCE) was largely shifted to a positive direction in the presence of Sc^{3+} (E_{red} = 0.31 V vs SCE) and Mg^{2+} (E_{red} = −0.05 V vs SCE). The E_{red} values in the presence of metal ions, determined by the differential pulse voltammograms in deaerated MeCN at 298 K, remain the same in the concentration range 3.3×10^{-3} to 4.0×10^{-1} M, when all PTQ molecules form the complexes with metal ions.

(38) The spectral titration of PTQ with metal ions (M^{n+} = Sc^{3+} and Mg^{2+}) indicates that PTQ forms 2:1 complexes with metal ions which bind with two PTQ molecules (PTQ−M^{n+}−PTQ). On the other hand, $PTQ^{\bullet-}$ forms 1:1 complexes with metal ions, as indicated by the ESR spectra in Figure 3. The further reduction of the 1:1 complexes between $PTQ^{\bullet-}$ and metal ions ($PTQ^{\bullet-}$−M^{n+}) may result in formation of 1:2 complexes between PTQ^{2-} and metal ions (M^{n+}−PTQ^{2-}−M^{n+}) rather than 1:1 complexes. In any case, the proportionation between PTQ and PTQ^{2-} in the presence of metal ions affords 1:1 complexes between $PTQ^{\bullet-}$ and metal ions. Such a change in the binding mode of metal ions depending on the redox state of PTQ as well as the detailed electron-transfer dynamics will be reported elsewhere.